


RESEARCH

Open Access



Comparison effects of *Ferula gummosa* essential oil and Beta-pinene Alginate nanoparticles on human melanoma and breast cancer cells proliferation and apoptotic index in short term normobaric hyperoxic model

Mahmoud Osanloo¹, Somayyeh Pishamad², Ali ghanbariasad³, Elham Zarenezhad⁴, Media Alipanah⁵ and Hiva Alipanah^{6*} 

Abstract

Background Breast cancer is the most common cancer among women, and melanoma is the most dreadful type of skin cancer. Due to the side effects of chemotherapy drugs, the development of new herbal nano-medicines has been considered.

Methods This study first investigated the chemical composition of *Ferula gummosa* essential oil using GC-MS analysis; β -pinene, with 61.57%, was the major compound. Next, alginate nanoparticles containing β -pinene and the essential oil with particle sizes of 174 ± 7 and 137 ± 6 nm were prepared. Meanwhile, their zeta potentials were 12.4 ± 0.7 and 28.1 ± 1 mV. Besides, the successful loading of β -pinene and the essential oil in nanoparticles was confirmed using ATR-FTIR analysis. After that, their effects on viability and apoptotic index of human melanoma and breast cancer cells were investigated in normoxia and normobaric hyperoxia (NBO) conditions.

Results The best efficacy on A-375 and MDA-MB-231 cells was achieved by alginate nanoparticles containing the EO at hyperoxic and normoxia conditions; IC_{50} 76 and 104 μ g/mL. Besides, it affected apoptosis-involved genes; as *Bax/Bcl-2* ratio was higher than 1, conditions for induction of apoptosis were obtained. Higher sensitivity was observed in the A-375 cell line treated with Alg-EO in the NBO model.

Conclusions Alginate nanoparticles containing *F. gummosa* EO could be considered for further investigation in anticancer studies. Also, it may be expected that NBO can be a new strategy for delaying cancer progression and improving nanotherapy efficacy.

Keywords Neoplasm, Nanotechnology, Melanoma, Breast Cancer, Hyperoxia

*Correspondence:

Hiva Alipanah
alipanah.hiwa@yahoo.com

Full list of author information is available at the end of the article



© The Author(s) 2023. **Open Access** This article is licensed under a Creative Commons Attribution 4.0 International License, which permits use, sharing, adaptation, distribution and reproduction in any medium or format, as long as you give appropriate credit to the original author(s) and the source, provide a link to the Creative Commons licence, and indicate if changes were made. The images or other third party material in this article are included in the article's Creative Commons licence, unless indicated otherwise in a credit line to the material. If material is not included in the article's Creative Commons licence and your intended use is not permitted by statutory regulation or exceeds the permitted use, you will need to obtain permission directly from the copyright holder. To view a copy of this licence, visit <http://creativecommons.org/licenses/by/4.0/>. The Creative Commons Public Domain Dedication waiver (<http://creativecommons.org/publicdomain/zero/1.0/>) applies to the data made available in this article, unless otherwise stated in a credit line to the data.

Introduction

Cancers, with 10 million deaths in 2020, were the leading cause of death worldwide; breast and skin cancer were among the five most common types [1]. Side effects of chemotherapeutic drugs have led researchers to develop new herbal drugs; essential oils (EOs) with anticancer effects are a proper alternative source [2]. EOs are naturally volatile oils secreted as secondary metabolites from different parts of aromatic plants such as roots, stems, leaves, and flowers. They also possess antioxidant, antibacterial, antitumor, and anti-leishmanial effects [3]. For instance, in the family of *Apiaceae*, *Ferula gummosa*, a perennial herb native to Iran and Turkmenistan, has been widely used in traditional medicine [4]. Its cytotoxic effects were reported on human malignant glioblastoma multiforme and oral squamous cell carcinoma cells [5, 6]. Interestingly, its gum induces apoptosis via the ROS mechanism in human leukemic cells [7]. Besides, its extracts inhibit angiogenesis in vitro [8]. Its anti-seizure, antibacterial, and insecticidal effects were also reported [9–11]. β -pinene is the major component of *F. gummosa* EO [12, 13]. Beta and alpha-pinene are well-known monoterpenes found in many EOs. They have various biological activities such as anticoagulant, antitumor, antimicrobial, antimalarial, antioxidant, anti-inflammatory, anti-leishmanial, and analgesic effects [14, 15].

Hypoxia, or the lack of difference between the amount of oxygen available and the percentage of oxygen utilization, usually occurs in cancer and ischemic heart diseases [16]. In cancer cells, the expression of genes with critical roles in angiogenesis, cell cycle, and metabolism is induced to adapt tumor cells to a hypoxic condition [17]. Hypoxia in the tumor is associated with increased tissue metastasis risk and decreased survival rate [18]. In addition, resistance to lack of oxygen as a pathophysiological property of solid tumors can reduce chemotherapy or radiation therapy efficacy and create a more malignant cancer phenotype [19]. In addition to in vitro studies, new research in animal and human models showed the different effects of hyperoxic treatment like hyperbaric hyperoxic (HBO) on burn injuries and tumor cells. In tissues suffering from wounds and burns, oxygen therapy causes faster tissue repair and saves cell death; oxygen enhancement in some cancer tissues has been associated with an increased apoptotic index of cancer cells [20, 21]. The dual behavior of non-cancerous and cancerous cells towards increased tissue oxygen is one of the most interesting biological phenomena. Won Kim et al. showed that normobaric hyperoxic (NBO) as another method of hyperoxic treatment did not show any significant hyperoxic damage in normal tissue and cells but suppressed the progression of lung cancer. In brief, they concluded that the therapeutic effect of NBO was probably due to the increase in reactive oxygen species activity and

apoptosis [22]. Besides, NBO is non-invasive and easier to administer than HBO [22]. Therefore, it is possible to consider and evaluate the increase of oxygen content as an adjuvant and promising therapeutic method to reduce tumor hypoxia and resistance to chemotherapy or radiation therapy.

Nowadays, herbal medicine is also expanding among cancer patients to treat or reduce the toxicity of chemotherapy drugs as a complementary treatment method [23, 24]. Despite the biodegradability and biocompatibility of herbal anticancer compounds (such as EOs and major compounds), their effectiveness is lower than synthetic drugs, and their solubility in water should also be improved [25, 26]. Including them in nanoparticles is proposed as a promising approach for the stability, solubility, and efficacy improvement of (herbal) drugs [27, 28]. Alginate is an anionic, biocompatible, and biodegradable polymer widely used in drug delivery [29, 30].

To the authors' best knowledge, no report was published on alginate nanoparticles containing *F. gummosa* EO and β -pinene. Besides, we evaluated the anticancer activity of nanoparticles containing *F. gummosa* EO and β -pinene on melanoma and breast cancer cells in the NBO model.

Materials and methods

A-375 (ATCC: CRL-1619) and MDA-MB-231 (ATCC: HTB-26) were bought from the Pasteur Institute of Iran. *F. gummosa* EO was purchased from Pharmaceutical Company Essential Oil Dr. Soleimani. Sodium alginate, calcium chloride, and β -pinene were provided from Sigma Aldrich (USA).

Identification of the chemical composition of *F. gummosa* EO

Identification of the chemical composition of *F. gummosa* EO was investigated using GC-MS analysis as described in our previous report [15]. The gas chromatography device used is Agilent 6890 with a column 30 m long, an inner diameter of 0.25 μ m, and a layer thickness of 0.25 μ m of BPX5 type. To identify the essential oil's components, the sample diluted by n-hexane was injected into the GC/MS machine in the amount of 1 μ l. The column temperature program was adjusted as follows: The initial temperature of the oven is 50 $^{\circ}$ C and remaining at this temperature for 5 min, thermal gradient of 3 $^{\circ}$ C/minute, increasing the temperature up to 240 degrees Celsius and then at a rate of 15 degrees per minute, increasing the temperature up to 300 $^{\circ}$ C and kept for 3 min at this temperature and the response time was 75 min (Fig. 1). The temperature of the injection chamber (port) is 250 $^{\circ}$ C in a split from 1 to 35, and helium gas was used as a carrier gas with a flow rate of 0.5 ml/min. The mass

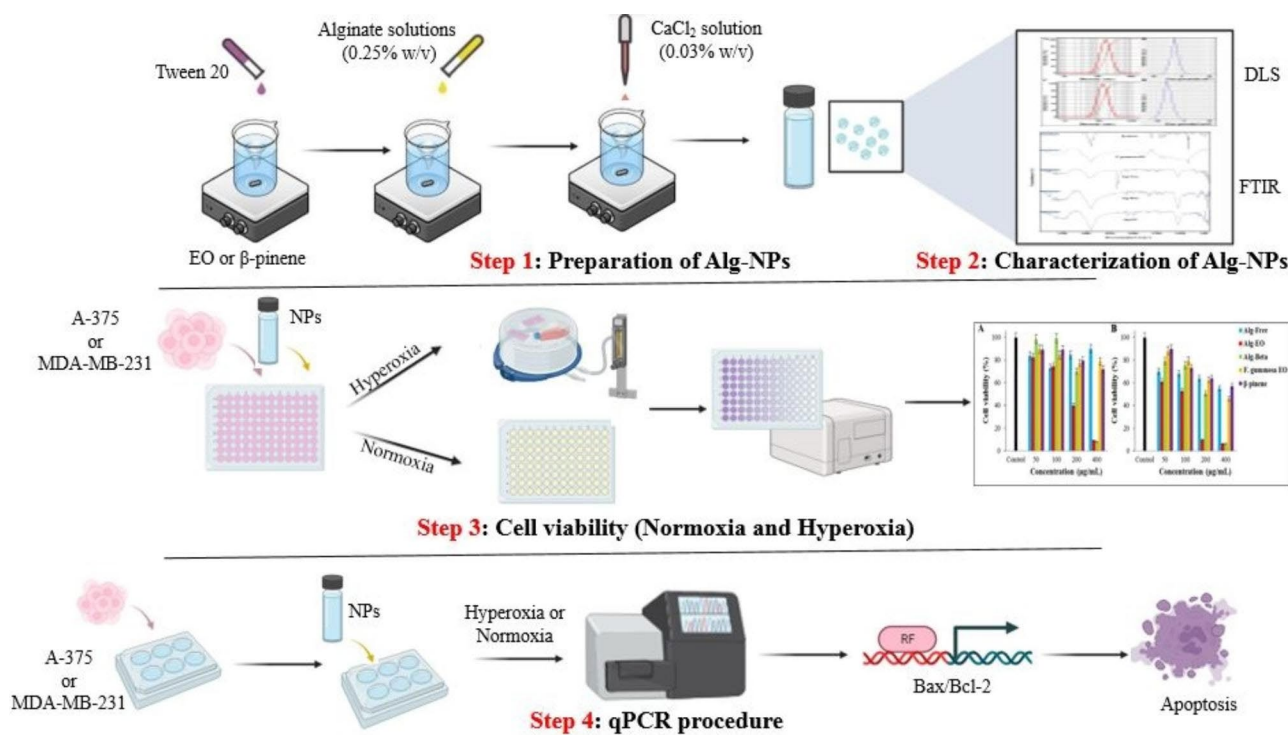


Fig. 1 Schematic diagram of the experimental methods. EO: Essential oil, NPs: nanoparticles

spectrometer was the Agilent 5973 model with an ionization voltage of 70 electron volts, EI ionization method, and ionization source temperature of 220 °C. The scanning range of mass spectrometry was adjusted from 40 to 500. The software used was Chemstation. The spectra were identified with the inhibition index and compared with those found in reference books and articles using the mass spectra of standard compounds and the information available in the computer library [31, 32].

Preparation and characterization of alginate nanoparticles containing *F. gummosa* EO and β -pinene

Ionic gelation was used to prepare alginate nanoparticles containing *F. gummosa* EO and β -pinene [33]. *F. gummosa* EO (0.16% w/v) or β -pinene (0.16% w/v) was first mixed with tween 20 (0.16% and 0.2% w/v, respectively) on magnetic stirrers (2000 rpm, RT), separately. Alginate solutions (0.25% w/v) were then added drop wisely and stirred for 5 min (2000 rpm, RT). After that, CaCl₂ solution (0.03% w/v) was added and stirred for 40 min (2000 rpm, RT). Besides, free alginate nanoparticles were also prepared in the same approach without β -pinene. The prepared free alginate nanoparticles and those containing *F. gummosa* EO and β -pinene were abbreviated as Alg-Free, Alg-EO, and Alg-Beta (Step 1, Fig. 1).

Particle size, particle size distribution (SPAN), and zeta potential of the as-prepared samples were investigated using DLS type apparatus. SPAN is calculated as $D_{90}-D_{10}/D_{50}$, where D is diameter and X are percentiles of

nanoparticles with a lower diameter than these points. Moreover, ATR-FTIR analysis was used to confirm the loading of *F. gummosa* EO and β -pinene in nanoparticles. Spectra of *F. gummosa* EO, β -pinene, Alg-Free, Alg-EO, and Alg-Beta were recorded at 500–4000 cm^{-1} . The samples were subjected to the device without any modification.

Attenuated total reflectance-Fourier transform infrared (ATR-FTIR) spectroscopy is useful for determining functional groups in various compounds [34]. Analysis of ATR-FTIR (Bruker Company, Model Tensor II, USA) was used to confirm the presence of *F. gummosa* EO and β -pinene in the alginate nanoparticles; these spectra are recorded in the range of 400–4000 cm^{-1} (Step 2, Fig. 1).

MTT assay procedure

MTT assay was used to investigate the cytotoxic effects of Alg-EO and Alg-Beta [35]. They were first diluted in PBS in serial dilutions of 50–800 $\mu\text{g}/\text{mL}$. The cells (A-375 and MDA-MB-231) were cultured in DMEM media culture containing 10% v/v FBS and 1% v/v penicillin/streptomycin. The cells were seeded (10^4 cells/well) in 96-well plates and incubated at 37 °C, 21% O₂, and 5% CO₂ to reach 80±5% confluence. Next, liquid media were replaced with 50 $\mu\text{L}/\text{well}$ of fresh media culture. Afterward, by adding 50 $\mu\text{L}/\text{well}$ of serial dilutions, the cytotoxic effects of Alg-EO and Alg-Beta were investigated at 50, 100, 200, and 400 $\mu\text{g}/\text{mL}$. Control group wells were treated with the used solvent (50 μL PBS), and

the negative control group was treated with Alg-Free. Treated plates were incubated for 24 h at normal and hyperoxia conditions. Next, 50 μL /well of MTT solution (0.5 mg/m/L) was added, and plates were incubated for 4 h at normal and Hyperoxic conditions (The chamber was flushed with 60% oxygen at normal pressure). After that, liquid media was discarded, and 200 μL /well of DMSO was added to dissolve formazan crystals. OD of wells was read at 570 nm using a plate reader, and cell viability was calculated by $\text{OD sample} / \text{OD control} \times 100$ (Step 3, Fig. 1).

The tests were performed three times, and the results are given as mean and standard deviations. IC_{50} values of samples were calculated using the free version of CalcuSyn.

qPCR procedure

This study investigates the impact of β -pinene, *F. gummosa* EO, Alg-Beta, and Alg-EO on the expression of *Bax* and *Bcl-2* genes in A-375 and MDA-MB-231 cell lines using the qPCR technique [36]. Briefly, 50,000 cells per well were distributed onto 6-well plates and subjected to an overnight incubation period under the specified conditions. Subsequently, samples with obtained IC_{50} concentration was introduced into the designated wells and subjected to a 24-hour incubation period at normal and hyperoxia condition. The extraction of total RNAs from cells was performed using the Trizol RNA extraction Kit. Subsequently, an assessment was conducted to determine the quality and amount of the extracted RNA. This evaluation used the Nano-drop instrument (SYNERGY, HTX, multi-mode reader, BioTek Instruments, USA). The purity of the RNA and the presence of protein contamination were confirmed by ensuring that the OD ratio at 260 and 280 nm exceeded 1.8.

The synthesis of complementary DNA (cDNA) was carried out per the methods provided by the manufacturer. In summary, obtained total RNAs were combined with oligo dT and DEPC water and subjected to incubation at temperatures of 70 °C and 4 °C for 5 and 1-minute durations, respectively. Subsequently, a strand buffer with a concentration of 5X, deoxyribonucleotide triphosphates (dNTPs), ribonuclease inhibitor (RNasin), and Moloney Murine Leukemia Virus Reverse Transcriptase (M-MLV) were introduced. Subsequently, the microtubes underwent thermal cycling using a T100 thermocycler system

manufactured by BIO-RAD in Germany. The thermal program was configured to run for a duration of 60 min at a temperature of 42 °C. The resulting complementary DNAs (cDNAs) were then stored at -20 °C.

The qPCR assay was conducted to examine the apoptotic regulatory genes *Bax* and *Bcl-2* and the expression of β -actin, which serves as a housekeeping gene. The primer sequences are provided in Table 1. To perform the amplification, a master mix containing forward and reverse primers, synthesized cDNA, and DEPC water (10, 0.5, 0.5, 1, and 8 μL , respectively) was prepared and transferred to a microtube. The microtube was then placed in an RT-PCR device (Step One Plus Real-Time PCR machine, AB Applied Biosystems, Germany). The normalization process employed Eq. $2^{-\Delta\Delta\text{CT}}$, and the obtained data was presented as fold change relative to the control cells (Step 4, Fig. 1).

Statistical analysis

Statistical analysis of data (mean \pm SD) was performed by one-way ANOVA using SPSS software with a confidence interval of 95%. Significance differences ($p < 0.05$) between the means evaluated by Tukey's multiple comparison tests. The IC_{50} values were calculated using CalcuSyn software (Free version, BIOSOFT, UK).

Results

Chemical compositions of *F. gummosa* EO

Identified compounds in *F. gummosa* EO are listed in Table 2. β -pinene, 4,6-Guaiadinene, guaiol, bulnesol, and α -pinene with 61.57, 5.43, 5.28, 5.05, and 3.46% are five major compounds.

Particle size and zeta potential of Alg-EO and Alg-Beta

DLS and zeta potential diagrams of Alg-Beta with a particle size of 174 ± 7 nm, SPAN 0.94, and zeta potential 12.4 ± 0.7 mV are shown in Fig. 2A and B. Besides, these diagrams for Alg-EO are depicted in Fig. 2 C and D; particle size 137 ± 6 nm, SPAN 0.95, and zeta potential 28.1 ± 1 mV.

Successful loading of β -pinene and *F. gummosa* EO in alginate nanoparticles

FTIR spectra of β -pinene showed that the bands at 3070 cm^{-1} attributed to =C-H stretching vibration and that at 2978, 2918, and 2868 cm^{-1} display -CH stretching vibration. The peak at 1640 and 1442 cm^{-1} corresponds to the C=C skeleton vibration. The peak at 1053 cm^{-1} is related to C-H bending absorption. The peak at 903 cm^{-1} can be attributed to the vibration absorption of alkenes. The band at 717 cm^{-1} is related to out-of-plane in C-H bending (Fig. 3).

ATR-FTIR spectrum of *F. gummosa* EO displayed the broad band between 3330 and 3690 cm^{-1} attributed

Table 1 Examined genes and their sequence

β-actin	Forward: 5' - TCCTCCTGAGCGCAAGTAC - 3' Reverse: 5' - CCTGCTTGCTGATCCACATCT - 3'
Bax	Forward: 5' - CCCGAGAGGTCTTTTCCGAG - 3' Reverse: 5' - CCAGCCCATGATGGTTCTGAT - 3'
Bcl-2	Forward: 5' - GGTGGGTCATGTGTGTGG - 3' Reverse: 5' - CGGTTCCAGGTACTCAGTCATCC - 3'

Table 2 Identified compounds in *F. gummosa* EO using GCMS analysis

NO	Re- ten- tion Time	%	Components	Kovats Index	Type
1	10.93	0.16	α -thujene	930	NH
2	11.31	3.46	α-pinene	939	NH
3	12.19	0.14	camphene	954	NH
4	13.38	0.39	sabinene	975	NH
5	13.69	61.57	β-pinene	979	NH
6	14.21	2.38	myrcene	991	NH
7	15.19	1.25	δ-Caren	1002	NH
8	16.19	0.19	<i>para</i> -Cymene	1025	NH
9	16.34	0.56	limonene	1029	NH
10	16.45	0.38	β -phellandrene	1030	NH
11	16.68	0.73	α -ocimene	1037	NH
12	17.23	0.22	β -ocimene	1050	NH
13	23.79	0.32	1,3,5-undecatriene	1165	other
14	24.27	0.60	1,2,5-undecatriene	1185	other
15	25.07	0.22	myrtenol	1196	MO
16	29.06	0.27	bornyl acetate	1289	MO
17	31.88	0.78	terpinene-4-ol-acatate	1300	MO
18	32.77	0.1	cyclosativene	1371	SH
19	33.03	0.17	α -Copaene	1377	SH
20	33.63	0.09	β -Elemene	1391	SH
21	34.98	0.16	caryophyllene E	1419	SH
22	37.71	0.77	aromadendrene	1441	SH
23	38.32	0.13	α -muurolene	1500	SH
24	39.09	0.12	δ -cadinene	1523	SH
25	40.43	0.63	elemol	1550	SH
26	42.33	5.28	guaiol	1601	SO
27	44.40	0.2	asarone	1617	MO
28	44.70	0.8	β -Eudesmol	1651	SO
29	44.99	5.43	4,6-Guaiadiene	1672	SO
30	45.71	5.05	bulnesol	1720	SH
31	46.53	0.73	valencene	1768	SO

MH: Monoterpene Hydrocarbons, MO: Oxygenated monoterpenes, SH: Sesquiterpene Hydrocarbon, SO: Oxygenated sesquiterpene

to the presence of OH group due to hydrogen bonding in the phenolic compound. The band at 2920 cm^{-1} is attributed to C-H stretching. The peak at 1735 cm^{-1} corresponded to C=O stretching that exhibited ester groups. The band at about 1457 cm^{-1} is allocated to CH_2 bending. The sharp band at 1103 cm^{-1} is related to C-O stretching vibration. ATR-FTIR spectrum of blank showed the broad band between 3200 and 3600 cm^{-1} are related to OH group due to hydrogen bonding in water and tween. The characteristic peak at 2922 cm^{-1} displayed CH stretching vibration in tween, the bands at 2341 and 2555 cm^{-1} can be related to CO_2 , and the peak at 1700 cm^{-1} can be attributed to the carbonyl group in tween 20. The strong band at about 1076 cm^{-1} can be related to C-O stretching in tween 20 (Fig. 3).

The ATIR spectra of alginate nanoparticles containing β -pinene displayed the broadband at about 3200–3700 cm^{-1} , related to OH groups, due to hydrogen bonding in water and tween, the band at 2923 cm^{-1} can be attributed to C-H stretching vibration, the band at 1772 cm^{-1} confirmed that the present of tween 20. The 1558 and 1351 cm^{-1} peaks corresponded to carbonyl groups' symmetric and asymmetric stretching vibration. The appearance of the other bands in the β -pinene and nanoparticles confirmed the successful loading of the β -pinene in the prepared nanoformulation.

The ATIR spectra of alginate nanoparticles containing *F. gummosa* EO showed a broad peak at about 3200–3700 cm^{-1} , attributed to hydroxyl groups, due to hydrogen bonding between EO, tween 20, and water, the band at 2959 cm^{-1} can be related to C-H stretching vibration, the peak at 1734 cm^{-1} demonstrated that the present of EO and tween 20. The bands at 1560 and 1352 cm^{-1} can be attributed to carbonyl groups' symmetric and asymmetric stretching vibration. The characteristic, strong peak at 1078 cm^{-1} in alginate nanoparticles containing β -pinene and *F. gummosa* EO confirmed the reaction between the carboxyl group and Calcium ion (CO-Ca-CO group structure), which increases C-O vibration. This characteristic band showed ionic crosslinking. The appearance of the other bands in the β -pinene or EO and alginate nanoparticles containing them confirmed the successful loading of the EO and β -pinene in the prepared nanoformulation (Fig. 3).

Cytotoxic effects of samples against A-375 and MDA-MB-231 cells

Cytotoxic effects of β -pinene and *F. gummosa* EO and their nanoformulated states (Alg-Beta and Alg-EO) against A-375 and MDA-MB-231 cells at normoxic and hyperoxic conditions represented as cell viability (Figs. 4 and 5) and IC_{50} values (Table 3). As shown in Fig. 4, exposure of A-375 cancer cells with 200 $\mu\text{g}/\text{ml}$ Alg-EO resulted in a substantial reduction ($\approx 50\%$) in cell viability compared with the control group. Cell viability in Alg-Beta, *F. gummosa* EO, and β -pinene groups demonstrated almost similar values upon treatment at 200 $\mu\text{g}/\text{ml}$ concentration. The results showed a dose-dependent manner in cancer A-375 cell proliferation upon treatment with Alg-Beta and Alg-EO. After 24h incubation with 400 $\mu\text{g}/\text{ml}$ of Alg-Beta and Alg-EO, cell proliferation reduced to below 20% in normoxic and hyperoxic conditions. The highest cytotoxic effect appeared after incubation with Alg-EO in the NBO condition with $\text{IC}_{50}=76 \mu\text{g}/\text{mL}$, where the IC_{50} value showed a 44% reduction compared to the normoxic condition (Table 3). As well as, treatment with the Alg-Beta, *F. gummosa* EO, and β -pinene in the NBO condition reduced IC_{50} values ($\approx 46\%$, 14%, and

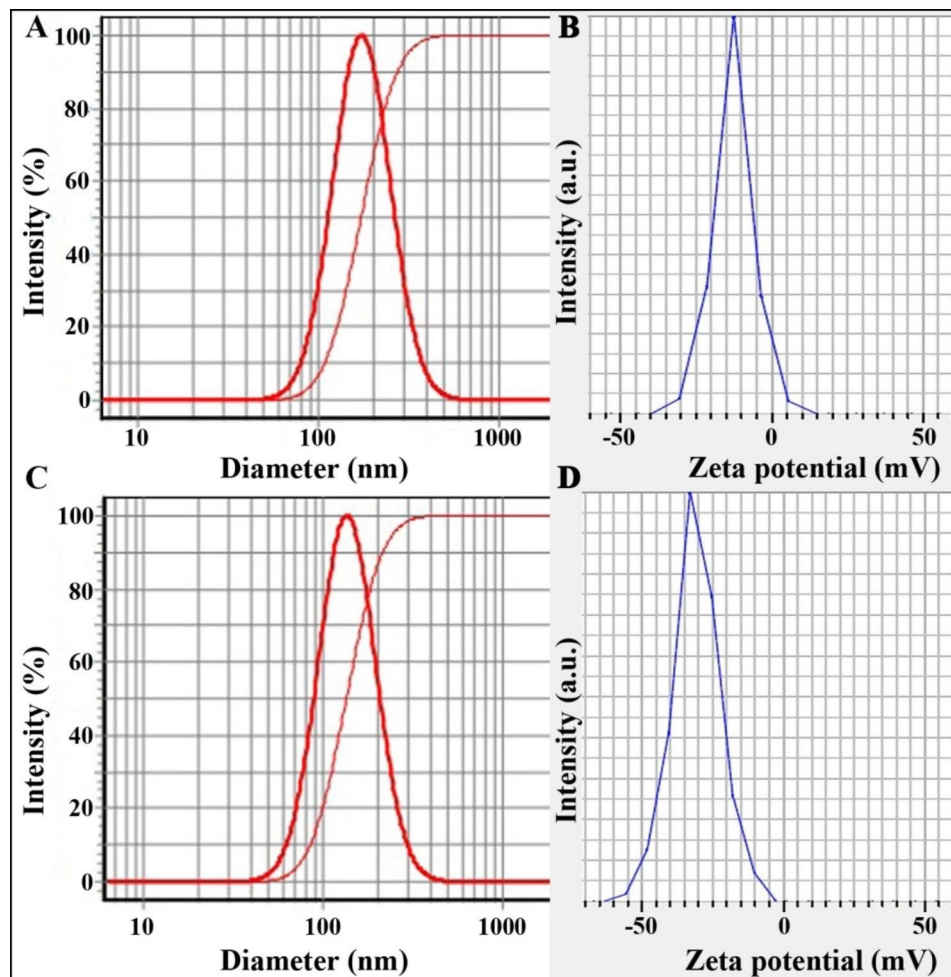


Fig. 2 DLS and zeta potential diagrams of Alg-Beta: (A) particle size 174 ± 7 nm and (B) zeta potential 12.4 ± 0.7 mV and Alg-EO: (C) particle size 137 ± 6 nm and (D) zeta potential 28.1 ± 1 mV

20%, respectively) compared with normoxic condition (Table 3).

As a result, at the end of 24h incubation, treatment with Alg-EO ($IC_{50}=104 \mu\text{g/mL}$) and Alg-Beta ($IC_{50}=142 \mu\text{g/mL}$) indicated relatively higher anticancer effect compared with their non-formulation ($IC_{50}=184$ and $323 \mu\text{g/mL}$, respectively) against MDA-MB-231 cells in normoxic condition (Fig. 5). In the NBO condition, regarding inhibition of cell proliferation, the cytotoxicity effects of Alg-EO and Alg-Beta were also more potent than their non-formulated states. It is important to note that the dose of Alg-beta ($142 \mu\text{g/mL}$) and β -pinene ($323 \mu\text{g/mL}$) to eradicate half population (50%) of MDA-MB-231 in normoxic was lower than in hyperoxic condition (205 and $536 \mu\text{g/mL}$, respectively). Results in Table 3 also showed that both cancer cell lines were more sensitive to Alg-EO and Alg-beta than their non-formulation in normoxic and hyperoxic conditions.

Prediction of cancer cell sensitivity with *Bax/Bcl-2* ratio

Effects of β -pinene, *E. gummosa* EO, Alg-Beta, and Alg-EO on *Bax* and *Bcl-2* gene expression in A-375 and MDA-MB-231 cells at normoxic and hyperoxic conditions are shown in Figs. 6 and 7. Cells were exposed to IC_{50} concentrations of the samples for 24 h and then analyzed for gene expression processing by qPCR (Figs. 6 and 7). Their *Bax/Bcl-2* ratio as an apoptotic index is summarized in Table 4. All samples at IC_{50} concentrations upregulated *Bax* (as a pro-apoptotic protein) in A-375 and MDA-MB-231 cancer cell lines in normoxic and hyperoxic models. The hyperoxic effect on overexpression of *Bax* in A-375 cells was more than normoxic condition. Also, a significant upregulation of *Bax* gene expression was observed in the Alg-EO and Alg-Beta nanoparticles groups compared to the control group. Our data also indicated that *Bcl-2* gene expression in A-375 cells was lower after treatment with Alg-EO and Alg-Beta in the NBO condition than normoxia. According to Table 4, Alg-EO and Alg-Beta increased apoptotic

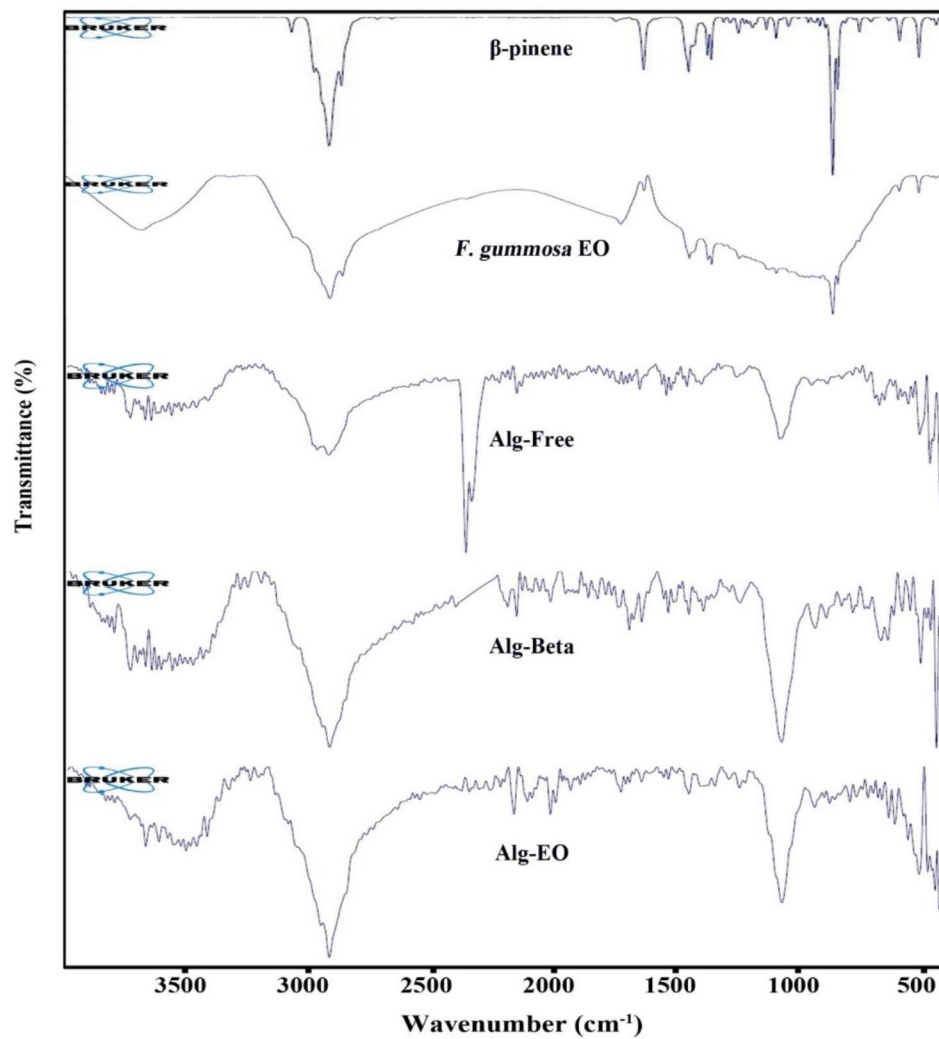


Fig. 3 ATR-FTIR of samples. Alg-EO: alginate nanoparticles containing *F. gummosa* EO, Alg-Beta: alginate nanoparticles containing β -pinene

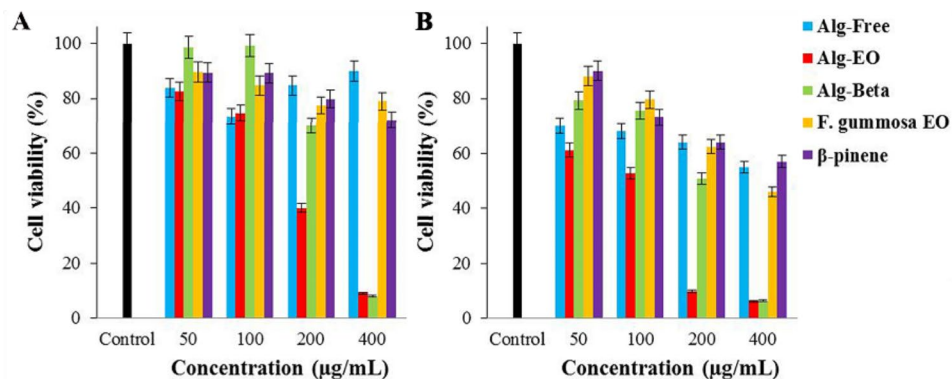


Fig. 4 Cytotoxic effects of samples on A-375 cells; (A) Normoxia and (B) Hyperoxic condition

index (*Bax/Bcl-2* ratio) in the A-375 cancer cell line in normoxia, but this ratio was higher in the NBO model. Higher sensitivity was observed in the A-375 cell line treated with Alg-EO in hyperoxic condition. Examining

the sensitivity of breast cancer cells to nanoparticles and hyperoxic showed that MDA-MB-231 cells are more sensitive to Alg-beta nanoparticles in normoxic and to Alg-EO nanoparticles in hyperoxic condition. The

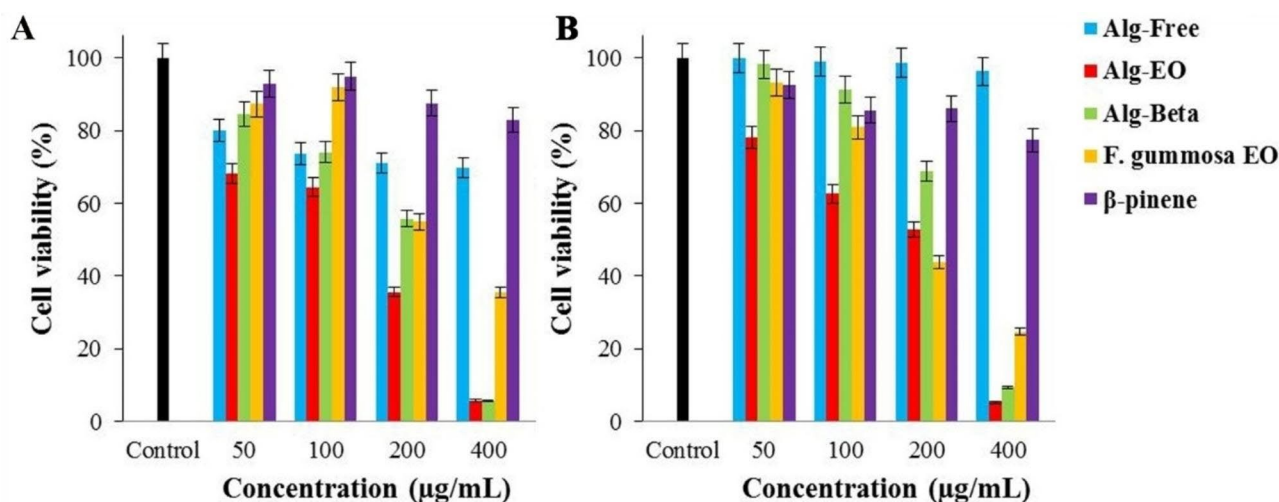


Fig. 5 Cytotoxic effects of samples on MDA-MB-231 cells; (A) Normoxic and (B) Hyperoxic condition. Alg-EO: alginate nanoparticles containing *F. gummosa* EO, Alg-Beta: alginate nanoparticles containing β -pinene

Table 3 Obtained IC_{50} (μ g/mL) values of samples against A-375 and MDA-MB-231 cells at normal and hyperoxic conditions

	A-375				MDA-MB-231			
	Normoxia		Hyperoxia		Normoxia		Hyperoxia	
	Alg-EO	Alg-Beta	<i>F. gummosa</i> EO	β -pinene	Alg-EO	Alg-Beta	<i>F. gummosa</i> EO	β -pinene
IC_{50}	136	248	262	302	76	132	226	242
	MDA-MB-231							
	Normoxia		Hyperoxia		Normoxia		Hyperoxia	
	Alg-EO	Alg-Beta	<i>F. gummosa</i> EO	β -pinene	Alg-EO	Alg-Beta	<i>F. gummosa</i> EO	β -pinene
IC_{50}	104	142	184	323	120	205	194	536

Alg-EO: alginate nanoparticles containing *F. gummosa* EO, Alg-Beta: alginate nanoparticles containing β -pinene

MDA-MB-231 cells showed the lowest sensitivity to β -pinene in normoxic and hyperoxic conditions.

Discussion

EOs as herbal remedies have been widely used in traditional medicine for a long time. Several in vitro and in vivo studies have explored the antibacterial, antifungal, anti-inflammatory, and anticancer properties of EOs [2, 37, 38]. Nevertheless, knowing the biological activities of phyto-components such as EOs and improving their effectiveness is part of the main goals of cancer and complementary medicine researchers. At first, GC-MS was applied in our study to determine the chemical compositions of *F. gummosa* EO. Then, alginate nanoparticles containing *F. gummosa* EO and its main compound, i.e., β -pinene, were evaluated to investigate their anticancer properties in normoxic and hyperoxic conditions. Several studies have also reported the main ingredients of *F. gummosa* EO. For example, GC-MS analysis of *F. gummosa* fruits, as noted by Ghasemi et al., demonstrated β -pinene (43.78%) as the major component [39]. Ghannadi et al. also reported the main components of gum and latex of *F.*

gummosa Boiss. grown in Iran was β -pinene (58.8%) [40]. Abbaszadegan et al. showed that β -pinene (51.83%) was the main compound of *F. gummosa* EO [41].

Laboratory and animal studies have shown that β -pinene has considerable antibacterial, antimalarial, antitumor, and gastro-protective effects. For example, Machado et al., by examining the anti-apoptotic effect of β -pinene against oral squamous cell carcinoma (OSCC), reported that β -pinene can be a possible new anticancer treatment for OSCC by inducing apoptotic index [42]. As well as a study was designed by Zhang et al. to investigate the combination of Paclitaxel and β -pinene against non-small-cell lung cancer cells and concluded that Paclitaxel and β -pinene have a synergistic anticancer effect [43]. In addition, in vitro analysis of the β -pinene anticancer effect on MCF-7 (breast cancer), A-375, and HepG2 (human hepatoma) cell lines done by Li et al. demonstrated antiproliferative activity of β -pinene against all cancer cell lines [44]. Alpha pinene is another terpenoid in *F. gummosa* EO with cancer-prevention properties. The therapeutic effect of α -pinene against prostate cancer (PC-3) growth was investigated by Zhao et al. in

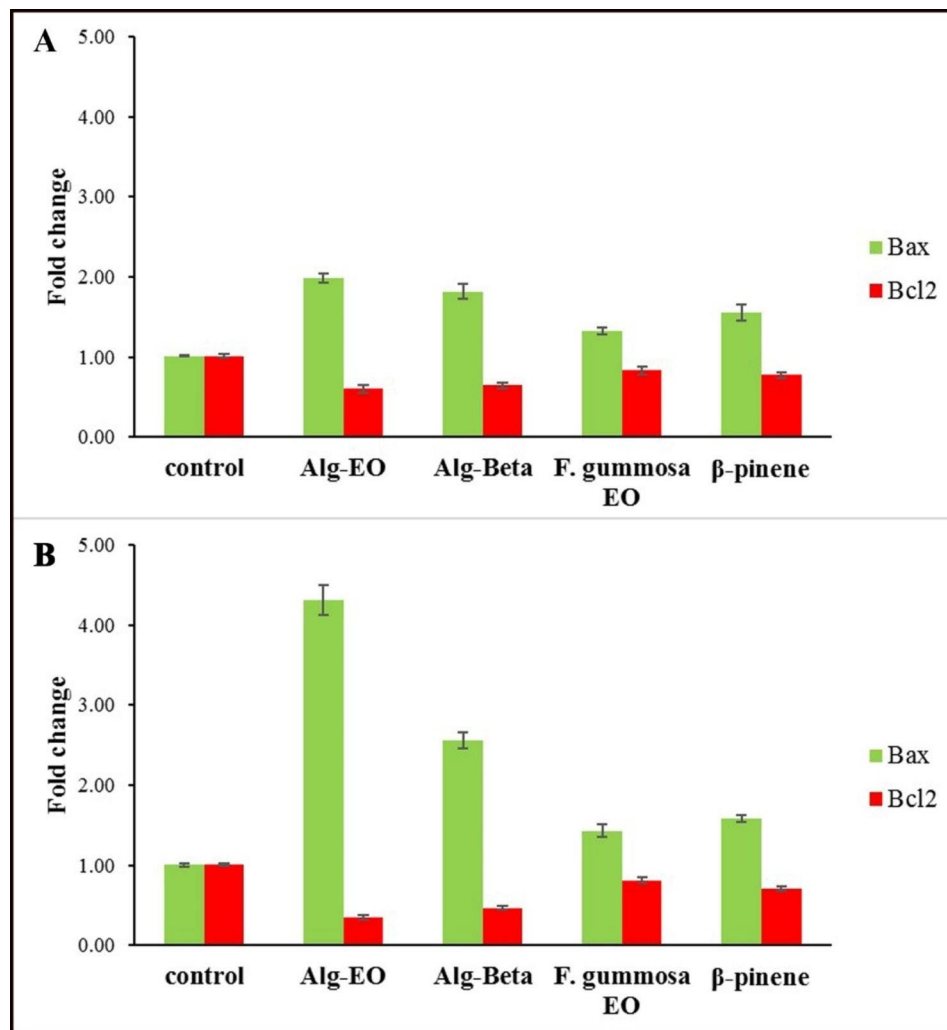


Fig. 6 Effects of samples on *Bax* and *Bcl-2* genes expression in A-375 cells; (A) Normoxic and (B) Hyperoxic condition. Alg-EO: alginate nanoparticles containing *F. gummosa* EO, Alg-Beta: alginate nanoparticles containing β-pinene

a xenograft model, which concluded that α-pinene had adverse toxicity on tumor progression and also induced cell cycle arrest and programmed cell death in PC-3 cell line [45]. Similarly, in a mice model, a fragrant environment enriched with α-pinene inhibited melanoma growth and reduced tumor volume by about 40% compared with the control group [46]. Inducing G2/M cell cycle arrest, inhibiting tumor invasion, and increasing the antitumor activity of natural killer cells are other anticancer mechanisms of alpha-pinene, which have been mentioned in the studies of Chen et al., Kang et al., and Jo et al. [43, 47].

Furthermore, *F. gummosa* EO can induce tumor cell death via multiple mechanisms like inducing apoptosis, inhibiting cell proliferation, and increasing cancer cells' absorption of chemotherapy drugs. For example, flow cytometry and annexin-V analysis, as Gudarzi et al. noted, demonstrated that ethanolic extract of *F.*

gummosa EO induced apoptosis and cell-cycle arrest in BHY cells (a human OSCC) [48]. These findings are congruent with results obtained by Gharaei et al., who reported that ethanol extracts of *F. gummosa* EO inhibited the cell proliferation of the human gastric cancer cell line, AGS, in a dose-dependent manner by inducing an apoptosis pathway [49]. Afshari et al. also evaluated the cytotoxicity of *F. gummosa* gum against U87 glioblastoma cells. Data indicated apoptogenic impacts of *F. gummosa* gum by upregulating of *Bax/Bcl-2* ratio [50]. Forouzmand et al. have explored the anticancer effects of *F. gummosa* in a radiation toxicity study against cervical cancer (Hela) cells and hypothesized that *F. gummosa* as a radiosensitizer agent had a synergistic effect with radiotherapy for inducing apoptosis in Hela cell [51]. Our in-vitro examination ensured *F. gummosa* EO and β-pinene anticancer impact, which was confirmed by the apoptotic index. Treatment with β-pinene showed

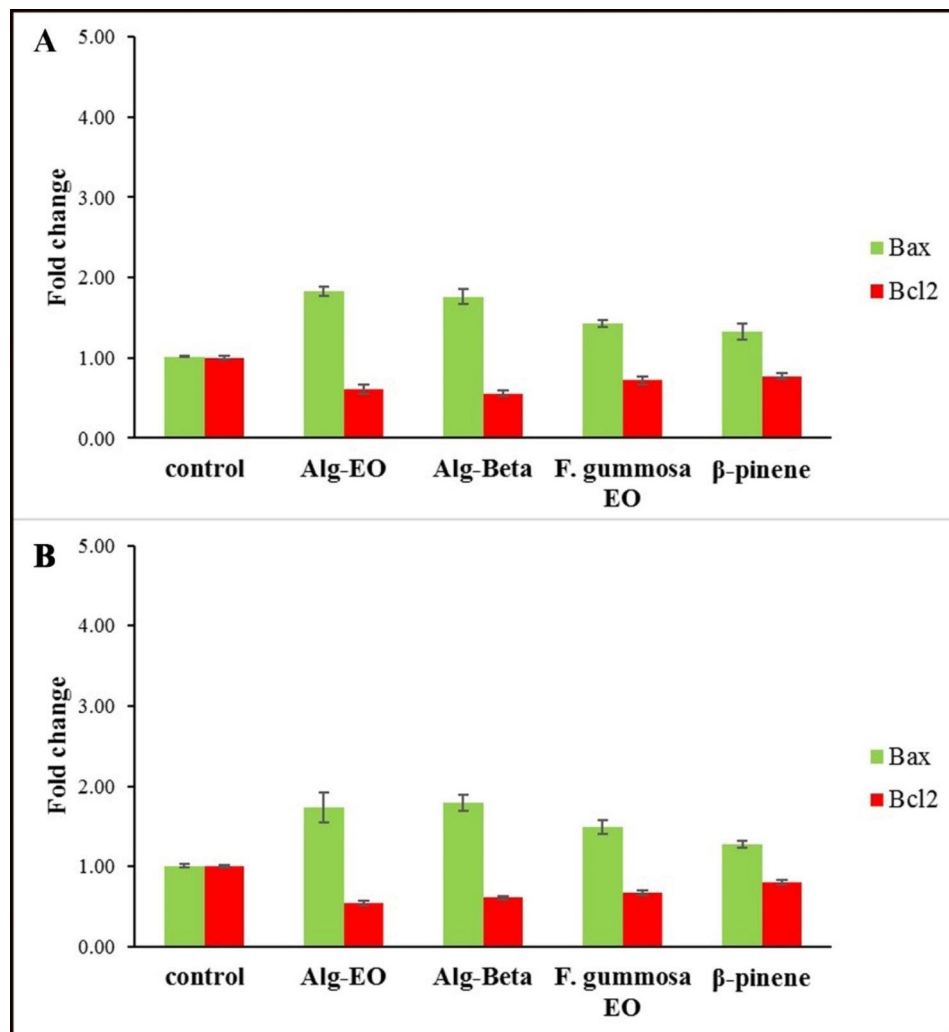


Fig. 7 Effects of samples on *Bax* and *Bcl-2* genes expression in MDA-MB-231 cells; (A) Normoxic and (B) Hyperoxic condition. Alg-EO: alginate nanoparticles containing *F. gummosa* EO, Alg-Beta: alginate nanoparticles containing β -pinene

a weak anticancer effect on A-375 ($IC_{50}=302 \mu\text{g/mL}$) and MDA-MB-231 ($IC_{50}=323 \mu\text{g/mL}$) cancer cells in normoxia condition, compared with *F. gummosa* EO ($IC_{50}=262 \mu\text{g/mL}$ and $184 \mu\text{g/mL}$ respectively). Because the nanoformulation of herbal medicines can increase their biological and pharmacological activities, we also used in vitro cancer models to evaluate AlgNPs containing *F. gummosa* EO and β -pinene. In vitro treatment of melanoma and breast cancer cells by AlgNPs markedly reduced cell viability percentages in cancer cells. Obtained IC_{50} for AlgNPs containing *F. gummosa* EO and β -pinene was significantly lower than non-formulation forms in both normoxia and hyperoxia conditions. Both cancer cell lines were the most sensitive to the anticancer effect of AlgNPs containing *F. gummosa* EO compared to Alg-Beta. From the literature, nanoemulsion from *F. gummosa* EO, as noted by Nosrat et al., can also reduce cell growth in the colon cancer model [52]. In addition,

treatment with chitosan-*F. gummosa* EO nanocomposite, as speculated by Valinezhad et al., showed stronger antibacterial activities [53]. The nanoformulation as a feasible strategy for improving anticancer properties of plant EOs is confirmed by various studies [54–56].

In addition, it has been well established that the presence of a hypoxic environment in solid tumors can increase the aggressive characteristics of cancer tumors by increasing the expression of various genes such as HIF-1 (hypoxia-inducible factor 1), VEGF (vascular endothelial growth factor), EGF (epidermal growth factor) and IGF-2 (insulin-like growth factor 2), followed by increased angiogenesis and tissue metastasis [57, 58]. Meanwhile, hypoxia can reduce the effectiveness of standard cancer therapy, such as chemotherapy and radiotherapy [57]. Oxygen therapy using NBO and HBO has been proposed as a therapeutic strategy to reverse tumor hypoxia. The anticancer activity of hyperoxia has also

Table 4 Correlation of cancer cell sensitivity to Alg-EO, Alg-Beta, *F. gummosa* EO, and β -pinene with *Bax/Bcl-2* ratio in normoxic and hyperoxic conditions

A-375 cells								
Sample	Normoxic				Hyperoxic			
	<i>Bax</i>	<i>Bcl-2</i>	<i>Bax/Bcl-2</i> ratio	Susceptibility*	<i>Bax</i>	<i>Bcl-2</i>	<i>Bax/Bcl-2</i> ratio	Susceptibility*
Alg-EO	1.99	0.60	3.31	+++	4.31	0.35	12.44	++++
Alg-Beta	1.82	0.65	2.81	++	2.56	0.46	5.53	+++
EO	1.32	0.83	1.58	+	1.43	0.81	1.75	+
β -pinene	1.56	0.78	2.00	+	1.58	0.71	2.23	++
MDA-MB-231 cells								
SAMPLES	Normoxic				Hyperoxic			
	<i>Bax</i>	<i>Bcl-2</i>	<i>Bax/Bcl-2</i> ratio	Susceptibility*	<i>Bax</i>	<i>Bcl-2</i>	<i>Bax/Bcl-2</i> ratio	Susceptibility*
Alg-EO	1.83	0.61	2.99	++	1.73	0.54	3.20	+++
Alg-Beta	1.76	0.56	3.17	+++	1.80	0.61	2.95	++
EO	1.43	0.72	2.00	+	1.49	0.67	2.24	++
β -pinene	1.33	0.77	1.72	+	1.27	0.80	1.59	+

Alg-EO: alginate nanoparticles containing *F. gummosa* EO, **Alg-Beta:** alginate nanoparticles containing β -pinene, **EO:** *F. gummosa* EO,

*A *Bax/Bcl-2* ratio < 1.00 characterizes cancer-resistant cells and a *Bax/Bcl-2* ratio > 1.00 cancer-sensitive cells.

+, low sensitivity (*Bax/Bcl-2* ratio 100–200% of control); ++, mild sensitivity (*Bax/Bcl-2* ratio 200–300% of control); +++, high sensitivity (*Bax/Bcl-2* ratio 300–600% of control), +++++, very high sensitivity (*Bax/Bcl-2* ratio > 600% of control).

been shown in laboratory and animal models; of course, the NBO method has received more attention than HBO because of its ease and fewer complications. Accordingly, our study evaluated the synergic effect of short-term NBO on the anticancer activity of Alg-EO and Alg-Beta against breast and melanoma cancer cells. Nanotherapy (Alg-EO and Alg-Beta) performed under NBO induced apoptosis and caused a considerable reduction in cell viability of A-375 cells with lower IC_{50} (76 and 132 $\mu\text{g}/\text{mL}$) compared with normoxia condition (136 and 248 $\mu\text{g}/\text{mL}$). It has been shown that hyperoxia with 60% oxygen can prevent the survival and proliferation of cancer cells by increasing oxidative stress and inducing apoptosis, and restoring the sensitivity to chemotherapy agents can provide the conditions for tumor regression [22, 59, 60]. This data is congruent with results obtained by Lee et al., who demonstrated hyperoxia re-sensitized human glioblastoma multiforme cells (D54 and U87) to temozolomide [61]. Similar to our results, the NBO condition, as noted by Kim et al., induced oxygen toxicity against the progression of lung cancer by inducing oxidative stress and apoptosis pathways [22]. Moon et al. showed that intermittent NBO alone or combined with carboplatin could be tumoricidal by induction of oxidative stress and apoptosis [62]. It has also been shown that, hyperoxia up to 60% O_2 increased lactate and intracellular acidification and significantly retarding tumor growth and metastasis in lung cancer [63]. In addition, Bels et al. also examined hyperoxia up to 60% O_2 against hematopoietic lymphoid cancer cell lines and had adverse inhibitory effects on leukemia cell proliferation [64]. Contrariwise, Tiron et al. indicated that the metastasis rate following long-term hyperoxia (80% O_2) increased in the 4T1 triple-negative breast cancer model [65]. Our examination also assured

that Alg-EO and Alg-Beta enhanced MDA-MB-231 breast cancer cell growth arrest, but hyperoxia (60% O_2) did not enhance this impact.

On the other hand, most of the previous studies on oxygen therapy have focused more on hyperbaric hyperoxia. For example, hyperbaric oxygen treatment, as noted by Chen et al., unlike non-hematopoietic (A549, MCF-7) cells, can induce apoptosis in hematopoietic (Jurkat, NCI-H929) cells [66]. Similarly, Granowitz et al. showed that HBO caused no increase in apoptotic index in the MCF7 human mammary adenocarcinoma cell line [67]. Moreover, Sun et al. also investigated the effect of HBO on human oral cancer and concluded that apoptosis showed no change after HBO therapy [68]. Hjelde et al. also investigated hyperoxia (400 kPa O_2) synergic effect on photodynamic therapy (PDT) on human colon carcinoma (SW480 and WiDr) and rat bladder cell carcinoma (AY-27) cell lines. They found that hyperbaric oxygen had no synergic effect on the photo-killing impact of PDT [69]. Following these findings, in most experimental and clinical studies, improved PDT outcomes have been established in hyperbaric oxygen-treated groups [70–72]. In addition, Kawasoe et al. reported that hyperbaric oxygen suppressed both tumor volume and number by enhancing carboplatin's chemotherapeutic effects in the osteosarcoma mice model [73]. Our data indicated that nanotherapy with Alg-EO and Alg-Beta modulate and block the cell viability in melanoma and breast cancer. Unlike the triple-negative breast cancer cell line (MDA-MB-231), normobaric hyperoxia in melanoma cells increased the anticancer effects of nanoparticles, which could be confirmed by increasing the apoptotic index. This disagreement may be due to different thresholds for apoptosis in cancer cells with different origins [66]. On

the other hand, the design and different hyperoxia conditions, duration of hyperoxia, and oxygen pressure can be the reasons for the differences observed in the mentioned studies. In addition, a more detailed investigation of apoptosis with live and dead staining (LDA) images and Ki-67 proliferation marker, IF staining along with DAPI and F-actin and also measuring the expression of different caspases can be helpful in discovering how cancer cells getting apoptotic following treatment with Alg-EO and Alg-beta.

Conclusion

The study evaluated the anticancer potential of alginate nanoparticles containing *Ferula gummosa* EO and β -pinene against melanoma and breast cancer cells under normoxic and hyperoxic conditions. Alg-EO and Alg-Beta induced apoptosis in melanoma and breast cancer cells confirmed by increased *Bax/Bcl-2* ratio. Our findings provide the first evidence that combination therapy with NBO enhanced apoptotic index in Alg nanoparticle-exposed melanoma cells, and it may be expected that NBO can be an alternative for cancer treatment. The study highlights the potential of combining natural herbal compounds with nanotechnology to improve their therapeutic efficacy, especially in conjunction with hyperoxic for cancer treatment.

Abbreviations

EO	Essential oil
Alg-EO	Alginate nanoparticles containing <i>F. gummosa</i> EO
Alg-Free	Free Alginate nanoparticles
Alg-Beta	Alginate nanoparticles containing β -pinene
NBO	Normobaric Hyperoxic
HBO	Hyperbaric Hyperoxic

Acknowledgements

None.

Authors' contributions

HA: Conceptualization, supervision, methodology. MO, HA, and MA were writing the original draft. MO and AGh: Software, validation, and data analysis. HA and SP: performed MTT assays. EZ interpreted ATR-FTIR. SP: Data curation and preparing nanoformulations. All authors contributed to drafting the manuscript and confirmed the final version.

Funding

Fasa University of Medical Sciences supported this study, Grant No. 401027.

Data Availability

The datasets used and/or analysed during the current study available from the corresponding author on reasonable request.

Declarations

Ethics approval and consent to participate

The study was approved by the Research Ethics Committee of Fasa University of Medical Sciences. Approval code: IR.FUMS.REC.1401.105.

Consent for publication

Not applicable.

Research involving humans and animals statement

This research did not involve human and animal studies.

Competing interests

The authors declare no competing interests.

Author details

¹Department of Medical Nanotechnology, School of Advanced Technologies in Medicine, Fasa University of Medical Sciences, Fasa, Iran

²Student Research Committee, Fasa University of Medical Sciences, Fasa, Iran

³Department of Medical Biotechnology, School of Advanced Technologies in Medicine, Fasa University of Medical Sciences, Fasa, Iran

⁴Noncommunicable Diseases Research Center, Fasa University of Medical Sciences, Fasa, Iran

⁵Faculty of Veterinary Medicine, Razi University, Kermanshah, Iran

⁶Department of Physiology, School of Medicine, Fasa University of Medical Sciences, Fasa, Iran

Received: 8 August 2023 / Accepted: 18 November 2023

Published online: 28 November 2023

References

1. WHO. Cancer Fact Sheet 2022 [cited 2023 June]. Available from: <https://www.who.int/news-room/fact-sheets/detail/cancer>.
2. Osanloo M, Yousefpoor Y, Alipanah H, Ghanbariasad A, Jalilvand M, Amani A. In-vitro Assessment of essential oils as Anticancer Therapeutic agents: a systematic literature review. *Jordan J Pharm Sci.* 2022;15(2):173–203. <https://doi.org/10.35516/jjps.v15i2.319>.
3. Noorpoor G, Ghadimi S, Sharifi N, Osanloo M. The leishmanicidal activity of essential oils: a systematic review. *J HerbMed Pharmacol.* 2020;9(4):300–8. <https://doi.org/10.34172/jhp.2020.38>.
4. Mahboubi M. *Ferula gummosa*, a Traditional Medicine with Novel Applications. *J Diet Suppl.* 2016;13(6):700–18. <https://doi.org/10.3109/19390211.2016.1157715>.
5. Afshari AR, Mousavi SH, Mousavi G, Moghadam SD, Maghrouni A, Javid H, et al. *Ferula gummosa* gum exerts cytotoxic effects against human malignant Glioblastoma Multiforme in vitro. *Res Pharm Sci.* 2022;17(5):585–93. <https://doi.org/10.4103/1735-5362.355215>.
6. Gudarzi H, Salimi M, Irian S, Amanzadeh A, Mostafapour Kandelous H, Azadmanesh K, et al. Ethanolic extract of *Ferula gummosa* is cytotoxic against cancer cells by inducing apoptosis and cell cycle arrest. *Nat Prod Res.* 2015;29(6):546–50. <https://doi.org/10.1080/14786419.2014.951854>.
7. Moradzadeh M, Sadeghnia HR, Mousavi SH, Mahmoodi M, Hosseini A. *Ferula gummosa* gum induces apoptosis via ROS mechanism in human leukemic cells. *Cell Mol Biol (Noisy-le-grand).* 2017;63(11):17–22. <https://doi.org/10.14715/cmb/2017.63.11.4>.
8. Mirzaaghaei S, Akrami H, Asadi MH, Mahdiani H. *Ferula gummosa* Boiss flower and leaf extracts inhibit angiogenesis in vitro. *Indian J Cancer.* 2014;51(4):615–20. <https://doi.org/10.4103/0019-509X.175323>.
9. Bashiri-Nahnjeh M, Sarihi A, Ebadi A, Dastan D, Mohammadi M. In silico molecular modeling, neuro-behavioral profile, and toxicity assessment of the essential oil of *Ferula gummosa* Boiss. As an anti-seizure agent. *J Ethnopharmacol.* 2023;309:116347. <https://doi.org/10.1016/j.jep.2023.116347>.
10. Najaf Najafi M, Arianmehr A, Sani AM. Preparation of Barije (*Ferula gummosa*) essential oil-loaded liposomes and evaluation of physical and antibacterial effect on *Escherichia coli* O157:H7. *J Food Prot.* 2020;83(3):511–7. <https://doi.org/10.4315/0362-028X.JFP-19-285>.
11. Pavela R, Morshedloo MR, Lupidi G, Carolla G, Barboni L, Quassinti L, et al. The volatile oils from the oleo-gum-resins of *Ferula assa-foetida* and *Ferula gummosa*: a comprehensive investigation of their insecticidal activity and eco-toxicological effects. *Food Chem Toxicol.* 2020;140:111312. <https://doi.org/10.1016/j.fct.2020.111312>.
12. Tabari MA, Youssefi MR, Nasiri M, Hamidi M, Kiani K, Alian Samakkhah S, et al. Towards green Drugs against cestodes: effectiveness of Pelargonium Roseum and *Ferula gummosa* essential oils and their main component on *Echinococcus Granulosus* protozoa. *Vet Parasitol.* 2019;266:84–7. <https://doi.org/10.1016/j.vetpar.2018.12.019>.

13. Abbaszadegan A, Gholami A, Mirhadhi H, Saliminasab M, Kazemi A, Moeini MR. Antimicrobial and cytotoxic activity of *Ferula gummosa* plant essential oil compared to NaOCl and CHX: a preliminary in vitro study. *Restor Dent Endod*. 2015;40(1):50–7. <https://doi.org/10.5395/rde.2015.40.1.50>.
14. Salehi B, Upadhyay S, Erdogan Orhan I, Kumar Jugran A, S LDJ DAD, et al. Therapeutic potential of α - and β -Pinene: a miracle gift of Nature. *Biomolecules*. 2019;9(11). <https://doi.org/10.3390/biom9110738>.
15. Rahmani H, Ghanbariasad A, Meshkibaf MH, Molazade A, Heiran R, Safari M, et al. Chitosan nanoparticles containing α -pinene and *Rosmarinus officinalis* L. essential oil: effects on human Melanoma cells' viability and expression of apoptosis-involved genes. *Polym Bull*. 2023. <https://doi.org/10.1007/s00289-023-04839-w>.
16. Carreau A, Hafny-Rahbi BE, Matejuk A, Grillon C, Kieda C. Why is the partial oxygen pressure of human tissues a crucial parameter? Small molecules and hypoxia. *J Cell Mol Med*. 2011;15(6):1239–53. <https://doi.org/10.1111/j.1582-4934.2011.01258.x>.
17. Ruan K, Song G, Ouyang G. Role of hypoxia in the hallmarks of human cancer. *J Cell Biochem*. 2009;107(6):1053–62. <https://doi.org/10.1002/jcb.22214>.
18. Hockel M, Vaupel P. Tumor hypoxia: definitions and current clinical, biologic, and molecular aspects. *J Natl Cancer Inst*. 2001;93(4):266–76. <https://doi.org/10.1093/jnci/93.4.266>.
19. Vaupel P, Mayer A, Höckel M. Tumor hypoxia and malignant progression. *Methods in enzymology*. Volume 381. Elsevier; 2004. pp. 335–54. [https://doi.org/10.1016/S0076-6879\(04\)81023-1](https://doi.org/10.1016/S0076-6879(04)81023-1).
20. Bhutani S, Vishwanath G. Hyperbaric oxygen and wound healing. *Indian J Plast Surg*. 2012;45(02):316–24. <https://doi.org/10.4103/0970-0358.101309>.
21. Sen S, Sen S. Therapeutic effects of hyperbaric oxygen: integrated review. *Med Gas Res*. 2021;11(1):30. <https://doi.org/10.4103/2045-9912.310057>.
22. Kim SW, Kim IK, Ha JH, Yeo CD, Kang HH, Kim JW, et al. Normobaric hyperoxia inhibits the progression of Lung cancer by inducing apoptosis. *Experimental Biology and Medicine*. 2018;243(9):739–48. <https://doi.org/10.1177/1535370218774737>.
23. Yang A-K, He S-M, Liu L, Liu J-P, Qian Wei M, Zhou S-F. Herbal interactions with anticancer Drugs: mechanistic and clinical considerations. *Curr Med Chem*. 2010;17(16):1635–78. <https://doi.org/10.2174/092986710791111279>.
24. Sparreboom A, Cox MC, Acharya MR, Figg WD. Herbal remedies in the United States: potential adverse interactions with anticancer agents. *J Clin Oncol*. 2004;22(12):2489–503. <https://doi.org/10.1200/JCO.2004.08.182>.
25. Colone M, Calcabrini A. Drug Delivery systems of Natural products. *In Oncology*. 2020;25(19). <https://doi.org/10.3390/molecules25194560>.
26. Cao J, Cao J, Wang H, Chen L, Cao F, Su E. Solubility improvement of phytochemicals using (natural) deep eutectic solvents and their bioactivity evaluation. *J Mol Liq*. 2020;318:113997. <https://doi.org/10.1016/j.molliq.2020.113997>.
27. Mitchell MJ, Billingsley MM, Haley RM, Wechsler ME, Peppas NA, Langer R. Engineering precision nanoparticles for drug delivery. *Nat Rev Drug Discov*. 2021;20(2):101–24.
28. Al-Dhubiab BE, Nair AB, Kumria R, Attimarad M, Harsha S. Formulation and evaluation of nano based drug delivery system for the buccal delivery of acyclovir. *Colloids Surf B Biointerfaces*. 2015;136:878–84. <https://doi.org/10.1016/j.colsurfb.2015.10.045>.
29. De S, Robinson D. Polymer relationships during preparation of chitosan-alginate and poly-L-lysine-alginate nanospheres. *J Control Release*. 2003;89(1):101–12. [https://doi.org/10.1016/s0168-3659\(03\)00098-1](https://doi.org/10.1016/s0168-3659(03)00098-1).
30. Paques JP, van der Linden E, van Rijn CJ, Sagis LM. Preparation methods of alginate nanoparticles. *Adv Colloid Interface Sci*. 2014;209:163–71. <https://doi.org/10.1016/j.cis.2014.03.009>.
31. Ibrahim M, Kainulainen P, Aflatuni A, Tiilikkala K, Adams R. Identification of Essential Oil Components by Gas Chromatography. *Controle Alternativo Da Antracnose Durante A PÓS-Colheita De Goiabas "Paluma" Simulando Armazenamento E A ComercializaçãO*. 2012:42.
32. McLafferty FW, Stauffer DB. *The Wiley/NBS registry of mass spectral data*. Wiley New York; 1989.
33. Valizadeh A, Hosseinzadeh M, Heiran R, Hatami S, Hosseiniour A, Osanloo M. Alginate nanoparticles containing *Lavandula angustifolia* essential oil as a potential potent, biocompatible and low-cost antitumor agent. *Polym Bull*. 2023. <https://doi.org/10.1007/s00289-023-04797-3>.
34. da Silva Bruni AR, de Oliveira VMAT, Fernandez AST, Sakai OA, Março PH, Valderama P. Attenuated total reflectance Fourier transform (ATR-FTIR) spectroscopy and chemometrics for organic cinnamon evaluation. *Food Chem*. 2021;365:130466. <https://doi.org/10.1016/j.foodchem.2021.130466>.
35. Rasti F, Yousefpoor Y, Abdollahi A, Safari M, Roozitalab G, Osanloo M. Antioxidative, anticancer, and antibacterial activities of a nanogel containing *Mentha spicata* L. essential oil and electrospun nanofibers of polycaprolactone-hydroxypropyl methylcellulose. *BMC Complement Med Ther*. 2022;22(1):261.
36. Azadi S, Osanloo M, Zarenezhad E, Farjam M, Jalali A, Ghanbariasad A. Nano-scaled emulsion and nanogel containing *Mentha pulegium* essential oil: cytotoxicity on human Melanoma cells and effects on apoptosis regulator genes. *BMC Complement Med Ther*. 2023;23(1):6. <https://doi.org/10.1186/s12906-023-03834-y>.
37. Kalembe D, Kunicka A. Antibacterial and antifungal properties of essential oils. *Curr Med Chem*. 2003;10(10):813–29. <https://doi.org/10.2174/0929867033457719>.
38. Pérez GS, Zavala SM, Arias GL, Ramos LM. Anti-inflammatory activity of some essential oils. *J Essent Oil Res*. 2011;23(5):38–44. <https://doi.org/10.1080/10412905.2011.9700480>.
39. Ghasemi Y, Faridi P, Mehregan I, Mohagheghzadeh A. *Ferula gummosa* fruits: an aromatic antimicrobial agent. *Chem Nat Compd*. 2005;41:311–4. <https://doi.org/10.1007/s10600-005-0138-3>.
40. Ghannadi A, Amree S. Volatile oil constituents of *Ferula gummosa* Boiss. From Khashan, Iran. *J Essent Oil Res*. 2002;14(6):420–1.
41. Abbaszadegan A, Gholami A, Mirhadhi H, Saliminasab M, Kazemi A, Moeini MR. Antimicrobial and cytotoxic activity of *Ferula gummosa* plant essential oil compared to NaOCl and CHX: a preliminary in vitro study. *Restor Dentistry Endodontics*. 2015;40(1):50–7. <https://doi.org/10.5395/rde.2015.40.1.50>.
42. Machado TQ, Felisberto JRS, Guimarães EF, Queiroz GAd F, ACCd, Ramos YJ, et al. Apoptotic effect of β -pinene on oral squamous cell carcinoma as one of the major compounds from essential oil of medicinal plant *Piper rivinoides* Kunth. *Nat Prod Res*. 2022;36(6):1636–40. <https://doi.org/10.1080/14786419.2021.1895148>.
43. Chen W, Liu Y, Li M, Mao J, Zhang L, Huang R, et al. Anti-tumor effect of α -pinene on human hepatoma cell lines through inducing G2/M cell cycle arrest. *J Pharmacol Sci*. 2015;127(3):332–8. <https://doi.org/10.1016/j.jpshs.2015.01.008>.
44. Li YLYC, Chiu LC, Cen YZ, Ooi VE. Chemical composition and antiproliferative activity of essential oil from the leaves of a medicinal herb, *Schefflera heptaphylla*. *Phytother Res*. 2009;23(1):140–2. <https://doi.org/10.1002/ptr.2567>.
45. Zhao Y, Chen R, Wang Y, Yang Y. α -Pinene inhibits human Prostate cancer growth in a mouse xenograft model. *Chemotherapy*. 2018;63(1):1–7. <https://doi.org/10.1159/000479863>.
46. Kusuvara M, Urakami K, Masuda Y, Zangiacomì V, Ishii H, Tai S, et al. Fragrant environment with α -pinene decreases Tumor growth in mice. *Biomed Res*. 2012;33(1):57–61. <https://doi.org/10.2220/biomedres.33.57>.
47. Kang E, Lee DH, Jung YJ, Shin SY, Koh D, Lee YH. α -Pinene inhibits Tumor invasion through downregulation of nuclear factor (NF)- κ B-regulated matrix metalloproteinase-9 gene expression in MDA-MB-231 human Breast cancer cells. *Appl Biol Chem*. 2016;59(4):511–6.
48. Gudarzi HSM, Irian S, Amanzadeh A, Mostafapour Kandelous H, Azadmanesh K, Salimi M. Ethanolic extract of *Ferula gummosa* is cytotoxic against cancer cells by inducing apoptosis and cell cycle arrest. *Nat Prod Res*. 2015;29(6):546–50. <https://doi.org/10.1080/14786419.2014.951854>.
49. Gharaei R, Akrami H, Heidari S, Asadi MH, Jalili A. The suppression effect of *Ferula gummosa* Boiss. Extracts on cell proliferation through apoptosis induction in gastric cancer cell line. *Eur J Integr Med*. 2013;5(3):241–7. <https://doi.org/10.1016/j.eujim.2013.01.002>.
50. Afshari AR, Mousavi SH, Mousavi G, Moghadam SD, Maghrouni A, Javid H, et al. *Ferula gummosa* gum exerts cytotoxic effects against human malignant Glioblastoma Multiforme in vitro. *Res Pharm Sci*. 2022;17(5):585. <https://doi.org/10.4103/1735-5362.355215>.
51. Forouzmand SHMS, Vazifedan V, Nourbakhsh M, Chamani J, Hoseini A, Fanipakdel A. Synergistic effects of *Ferula gummosa* and radiotherapy on induction of cytotoxicity in HeLa cell line. *Avicenna J Phytomedicine*. 2018;8(5):439.
52. Nosrat TTM, Etmīnan A, Irani M, Zarei B, Rahmati A. In vitro and in vivo anti-cancer activity of *Ferula gummosa* essential oil nanoemulsions (FGEO-NE) for the colon Cancer treatment. *J Polym Environ*. 2022;30(10):4166–77. <https://doi.org/10.1203/rs.3.rs-1324811/v1>.
53. Valinezhad NTA, Alamdari S. Biosynthesize, physicochemical characterization and biological investigations of chitosan-*Ferula gummosa* essential oil (CS-FEO) nanocomposite. *Int J Biol Macromol*. 2023;30(241):124503. <https://doi.org/10.41016/j.jbiomac.2023.124503>.
54. Valizadeh A, Khaleghi AA, Alipanah H, Zarenezhad E, Osanloo M. Anticarcinogenic effect of chitosan nanoparticles containing *syzygium aromaticum*

- essential oil or eugenol toward breast and Skin cancer cell lines. *BioNanoScience*. 2021;11(3):678–86. <https://doi.org/10.1007/s12668-021-00880-z>.
55. Al-Tawarah NM, Qaralleh H, Khlaifat AM, Nofal MN, Alqaraleh M, Khleifat KM, et al. Anticancer and antibacterial properties of verthemia iphionides essential oil/silver nanoparticles. *Biomed Pharmacol J*. 2020;13(3):1175–85. <https://doi.org/10.13005/bpj/1985>.
 56. Hosseinzadeh N, Shomali T, Hosseinzadeh S, Raouf Fard F, Pourmontaseri M, Fazeli M. Green synthesis of gold nanoparticles by using *Ferula Persica* Willd. Gum essential oil: production, characterization and in vitro anti-cancer effects. *J Pharm Pharmacol*. 2020;72(8):1013–25. <https://doi.org/10.1111/jphp.13274>.
 57. Kim SWKI, Lee SH. Role of hyperoxic treatment in cancer. *Experimental Biology and Medicine*. 2020;254(10):851–60. <https://doi.org/10.1177/1535370220921547>.
 58. Fechner GDF, Schmidt D, Müller S, Vaupel P, Albers P. Hyperoxia-induced improvement of the in vitro response to gemcitabine in transitional cell carcinoma. Hyperoxia-induced improvement of the in vitro response to gemcitabine in transitional cell carcinoma. *Anticancer Res*. 2005;1(25):3413–8.
 59. Hatfield SM, Kjaergaard J, Lukashev D, Belikoff B, Schreiber TH, Sethumadhavan S. Systemic oxygenation weakens the hypoxia and hypoxia inducible factor 1 α -dependent and extracellular adenosine-mediated tumor protection. *Journal of molecular medicine*. Hatfield SM, Kjaergaard J, Lukashev D, Belikoff B, Schreiber TH, Sethumadhavan S et al. Systemic oxygenation weakens the hypoxia and hypoxia inducible factor 1 α -dependent and extracellular adenosine-mediated tumor protection. *Journal of molecular medicine*. 2014;92:1283–92.
 60. Kim SW, Kim IK, Lee SH. Role of hyperoxic treatment in cancer. *Experimental Biology and Medicine*. 2020;245(10):851–60. <https://doi.org/10.1177/1535370220921547>.
 61. Lee D, Sun S, Ho AS, Kiang KM, Zhang XQ, Xu FF, et al. Hyperoxia resensitizes chemoresistant glioblastoma cells to temozolomide through unfolded protein response. *Anticancer Res*. 2014;34(6):2957–66.
 62. Lee HY, Kim IK, Lee HI, Lee HY, Kang HS, Yeo CD, et al. Combination of carboplatin and intermittent normobaric hyperoxia synergistically suppresses benzo [a] pyrene-induced Lung cancer. *Korean J Intern Med*. 2018;33(3):541. <https://doi.org/10.3904/kjim.2016.334>.
 63. Liu X, Qin H, Zhang L, Jia C, Chao Z, Qin X, et al. Hyperoxia induces glucose metabolism reprogramming and intracellular acidification by suppressing MYC/MCT1 axis in Lung cancer. *Redox Biol*. 2023;61:102647. <https://doi.org/10.1016/j.redox.2023.102647>.
 64. De Bels D, Tillmans F, Corazza F, Bizzarri M, Germonpre P, Radermacher P, et al. Hyperoxia alters ultrastructure and induces apoptosis in Leukemia cell lines. *Biomolecules*. 2020;10(2):282. <https://doi.org/10.3390/biom10020282>.
 65. Tiron A, Ristescu I, Postu PA, Tiron CE, Zugun-Eloae F, Grigoras I. Long-Term Deleterious Effects of Short-term Hyperoxia on Cancer Progression—Is Brain-Derived Neurotrophic Factor an Important Mediator? An Experimental Study. *Cancers*, Tiron A, Ristescu I, Postu PA, Tiron CE, Zugun-Eloae F, Grigoras I. Long-Term Deleterious Effects of Short-term Hyperoxia on Cancer Progression—Is Brain-Derived Neurotrophic Factor an Important Mediator? An Experimental Study. *Cancers*. 2020;12(3):688.
 66. Chen Y-C, Chen S-Y, Ho P-S, Lin C-H, Cheng Y-Y, Wang J-K, et al. Apoptosis of T-leukemia and B-myeloma cancer cells induced by hyperbaric oxygen increased phosphorylation of p38 MAPK. *Leuk Res*. 2007;31(6):805–15. <https://doi.org/10.1016/j.leukres.2006.09.016>.
 67. Granowitz EV, Tonomura N, Benson RM, Katz DM, Band V, Makari-Judson GP, et al. Hyperbaric oxygen inhibits benign and malignant human mammary epithelial cell proliferation. *Anticancer Res*. 2005;25(6B):3833–42.
 68. Sun T, Chen R, Hsu Y. The effect of hyperbaric oxygen on human Oral cancer cells. *Undersea & Hyperbaric Medicine*. 2004;31(2):251.
 69. Hjelde 1ABCDEFGA, Gederas ABCDEFGOA. Krokan2ADE HE, Brubbak1ADE AO. Lack of effect of hyperoxia on photodynamic therapy and lipid peroxidation in three different cancer cell lines. *Med Sci Monit*. 2005;11(10):356.
 70. Maier A, Anegg U, Fell B, Rehak P, Ratzenhofer B, Tomaselli F, et al. Hyperbaric oxygen and photodynamic therapy in the treatment of advanced carcinoma of the cardia and the esophagus. *Lasers in Surgery and medicine*. Official J Am Soc Laser Med Surg. 2000;26(3):308–15. [https://doi.org/10.1002/\(sici\)1096-9101\(2000\)26:3<308::aid-lsm9>3.0.co;2-b](https://doi.org/10.1002/(sici)1096-9101(2000)26:3<308::aid-lsm9>3.0.co;2-b).
 71. Dong G-c, Hu S-x, Zhao G-y, Gao S-z, Wu L-r. experimental study on cytotoxic effects of hyperbaric oxygen and photodynamic therapy on mouse transplanted Tumor. *Chin Med J*. 1987;100(09):697–702.
 72. Maier A, Tomaselli F, Anegg U, Rehak P, Fell B, Luznik S, et al. Combined photodynamic therapy and hyperbaric oxygenation in carcinoma of the esophagus and the esophago-gastric junction. *Eur J Cardiothorac Surg*. 2000;18(6):649–55. [https://doi.org/10.1016/s1010-7940\(00\)00592-3](https://doi.org/10.1016/s1010-7940(00)00592-3).
 73. Kawasoe Y, Yokouchi M, Ueno Y, Iwaya H, Yoshida H, Komiya S. Hyperbaric oxygen as a chemotherapy adjuvant in the treatment of osteosarcoma. *Oncol Rep*. 2009;22(5):1045–50. https://doi.org/10.3892/or_00000534.

Publisher's Note

Springer Nature remains neutral with regard to jurisdictional claims in published maps and institutional affiliations.